

Influence of interfacial roughness on exchange bias in core-shell nanoparticles

R. F. L. Evans, D. Bate, and R. W. Chantrell

Department of Physics, The University of York, York, YO10 5DD, United Kingdom

R. Yanes and O. Chubykalo-Fesenko

Instituto de Ciencia de Materiales de Madrid, CSIC, Cantoblanco, E-28049 Madrid, Spain

(Received 31 May 2011; revised manuscript received 4 August 2011; published 28 September 2011)

Exchange bias is a phenomenon that has attracted a great deal of interest in the 50 years following its discovery, but that is still lacking a deep theoretical understanding of its origin in core-shell nanoparticles. We present calculations of ferro-antiferromagnetic core-shell nanoparticles with roughened interfaces and demonstrate a wide dispersion in the calculated exchange-bias field caused by the roughening. Furthermore, we show that the magnitude of the exchange-bias field is strongly correlated with the net interfacial moment in the antiferromagnet, proportional to the degree of the interfacial roughness. This provides new insight into the origins of exchange bias in core-shell nanoparticles.

DOI: [10.1103/PhysRevB.84.092404](https://doi.org/10.1103/PhysRevB.84.092404)

PACS number(s): 75.75.-c, 75.10.Hk, 75.50.Tt, 75.70.Rf

Exchange bias was first discovered in 1956 by Meikeljohn and Bean¹ who found that oxidized cobalt nanoparticles exhibited a shift of the hysteresis loop under field cooling of the sample. Exchange-biased systems are still an active area of research today, partly due to their intrinsic complexity² and technological applications in magnetic read heads and potential future application in magnetic random access memory³ (MRAM). Renewed interest has recently been shown in core-shell exchange-bias systems due to their potential application in increasing the superparamagnetic limit of small magnetic nanoparticles used in data storage systems.^{4,5} Recent experimental⁶ and theoretical^{7,8} studies have provided added insight into the possible origins of exchange bias in core-shell nanoparticles, however, the origins of the diversity of the experimentally observed behavior is still an unsolved problem. Particularly, the control of the exchange-bias phenomenon is difficult to achieve due to the important contribution of the magnetic frustration associated with the interface.⁹ The principal ingredients leading to this effect are the existence of uncompensated spins and/or interface roughness.^{10,11} While the first idea is implemented in many theoretical models, most of the roughness effects have been investigated theoretically in thin film systems,^{10,12} and not in core-shell nanoparticles, despite their potential significance.^{9,13,14}

In previous theoretical studies^{7,8} the calculated exchange bias is shown to vary with different shell thickness and particle size, but this in itself does not account for the observed experimental results. In order to observe exchange bias in the previous studies, very high anisotropies in the shell were required, being a significant fraction of the exchange energy, which is probably nonphysical; such large anisotropies are not observed experimentally. The exchange bias was attributed to the presence of net magnetic moment at the interface.¹⁵ This net magnetic moment was created in the antiferromagnetic shell by quenching of the spin directions for low temperature and a large anisotropy value. The use of more realistic CoO anisotropy parameters show that the resulting exchange-bias values are in this case very small.

An alternative approach is to add a roughened interface, which gives rise to a net interfacial moment (as in the present work), and/or allow for more realistic anisotropy in the shell,

but lower the interfacial exchange energy to a small fraction of the bulk as in Ref. 5.

In this work we present calculations of the hysteretic properties of a collection of core-shell nanoparticles with roughened interfaces between the ferromagnetic core and antiferromagnetic shell, representative of the Co-CoO systems found in Refs. 1 and 6, specifically looking at the role of the interface roughness on the exchange-bias field.

Given that antiferromagnetism is an atomic scale phenomenon, we have utilized a classical atomistic spin model to describe the magnetic properties of the system. In order to model core-shell ferromagnetic-antiferromagnetic (FM-AFM) nanoparticles, we have used a Heisenberg spin Hamiltonian which describes the energetics of a ferromagnetic (FM) core and antiferromagnetic (AFM) shell, respectively, given by

$$\mathcal{H} = \mathcal{H}_{\text{fm}} + \mathcal{H}_{\text{afm}}, \quad (1)$$

$$\begin{aligned} \mathcal{H}_{\text{fm}} = & \sum_{i,j} J_{\text{fm}} \mathbf{S}_i \cdot \mathbf{S}_j + \sum_{i,v} J_{\text{fm-afm}} \mathbf{S}_i \cdot \mathbf{S}_v \\ & - K_{\text{fm}} \sum_i (S_i^z)^2 - \mu_{\text{fm}} \sum_i \mathbf{H}_{\text{app}} \cdot \mathbf{S}_i, \end{aligned} \quad (2)$$

$$\begin{aligned} \mathcal{H}_{\text{afm}} = & \sum_{v,\delta} J_{\text{afm}} \mathbf{S}_v \cdot \mathbf{S}_\delta + \sum_{v,j} J_{\text{fm-afm}} \mathbf{S}_v \cdot \mathbf{S}_j \\ & - K_{\text{afm}} \sum_v (S_v^z)^2 - \mu_{\text{afm}} \sum_v \mathbf{H}_{\text{app}} \cdot \mathbf{S}_v, \end{aligned} \quad (3)$$

where \mathbf{S} is the spin unit vector, i, j label ferromagnetic sites with moment μ_{fm} , and v, δ label antiferromagnetic sites with moment μ_{afm} . $J_{\text{fm}} = -11.2 \times 10^{-21}$ J/link is the ferromagnetic exchange interaction, $J_{\text{afm}} = 4.2 \times 10^{-21}$ J/link is the antiferromagnetic exchange interaction, $J_{\text{fm-afm}}$ is the interfacial exchange interaction, K_{fm} is the ferromagnetic uniaxial anisotropy constant, K_{afm} is the antiferromagnetic uniaxial anisotropy constant, and \mathbf{H}_{app} is the external applied field. The parameters used closely resemble those of a Co-CoO core-shell system, with a Curie temperature for the FM of 1390 K¹⁶ and a Néel temperature for the AFM of 400 K.¹ The anisotropy in the FM (K_{fm}) was set to 4.644×10^{-24} J/atom¹⁷ and $K_{\text{afm}} = 10K_{\text{fm}}$. The exchange parameters are derived from the Curie point (FM) and Néel temperature (AFM) for the

system using the mean-field exchange value from the relation:

$$J_{ij} = \frac{3k_B T_c}{\epsilon z}, \quad (4)$$

where z is the coordination number of the lattice and $\epsilon = 0.8$ is a correction to the mean-field Curie point to account for the deviation arising due to spin-spin correlations.¹⁸ The interfacial exchange between the core and shell, $J_{\text{fm-afm}}$, was set at 5.6×10^{-22} J/link, which provides weak coupling between the core and shell.

The spherical core-shell particles are cut from a simple cubic crystal lattice. The total size of the particle is 5 nm in diameter with an initial inner core region of 4 nm in diameter. The particles are cut with an atom located at the center, ensuring that by default the particle has an uncompensated interface, where a net real magnetic moment exists in the AFM. In order to introduce interface roughness while avoiding excessive intermixing (many isolated core atoms) we have adopted the following approach. A spherical volume of radius greater than the total particle radius is first subdivided into small pyramidal volume elements, with 1 deg resolution. Each element is then assigned a random local radius of $r + \delta r$, where r is the radius of the core and δr is generated from a standard Gaussian random number and multiplied by a fractional radius, in our case 5%, corresponding to approximately one lattice spacing. Each atom in the particle is then allocated to the core or shell according to the local radius defined in the appropriate volume element. The individual structure of the particle can then be altered by using a different seed for the Gaussian random number. Sample visualizations of the generated particles are shown in Fig. 1, black signifying the core (FM) atoms, and white signifying the shell (AFM) atoms. The time evolution of the system is modeled with the Landau-Lifshitz-Gilbert (LLG) equation with Langevin dynamics^{19,20} with an intrinsic damping constant of 1.0 and time step of 5×10^{-16} s. The system is integrated using the Heun integration scheme¹⁹ and the external applied field is cycled to generate a single hysteresis loop for each particle.

Due to the variation in the roughened interfaces, the bias direction is unknown *a priori*, and so some form of setting procedure is required. One approach is to quench the system from high temperature in a strong applied field, though to ensure reliable setting the cooling must be performed reasonably slowly, which is computationally intensive. Therefore we have adopted an alternative approach where the exchange bias is set using the following energy minimization procedure. The (FM) core atoms are first oriented along the $+z$ direction, indicating the desired core orientation at positive field saturation. The AFM shell is then set with one of two polarities, AFM+ and AFM-, indicating whether alternate atoms in the lattice are up-down-up-down or down-up-down-up. For each of the polarities the total system energy is calculated, and the polarity with the lowest energy is then selected. This process ensured a left shift of the hysteresis loop for all particles, consistent with the setting of a fully saturated exchange-bias system.

In order to calculate the exchange-bias field of such particles we have calculated hysteresis loops at a temperature of 10 K for 128 particles, each with a different interface. The hysteresis loops are calculated at a field rate of 2 T/ns, and the exchange-bias field is calculated as the mean of the forward and

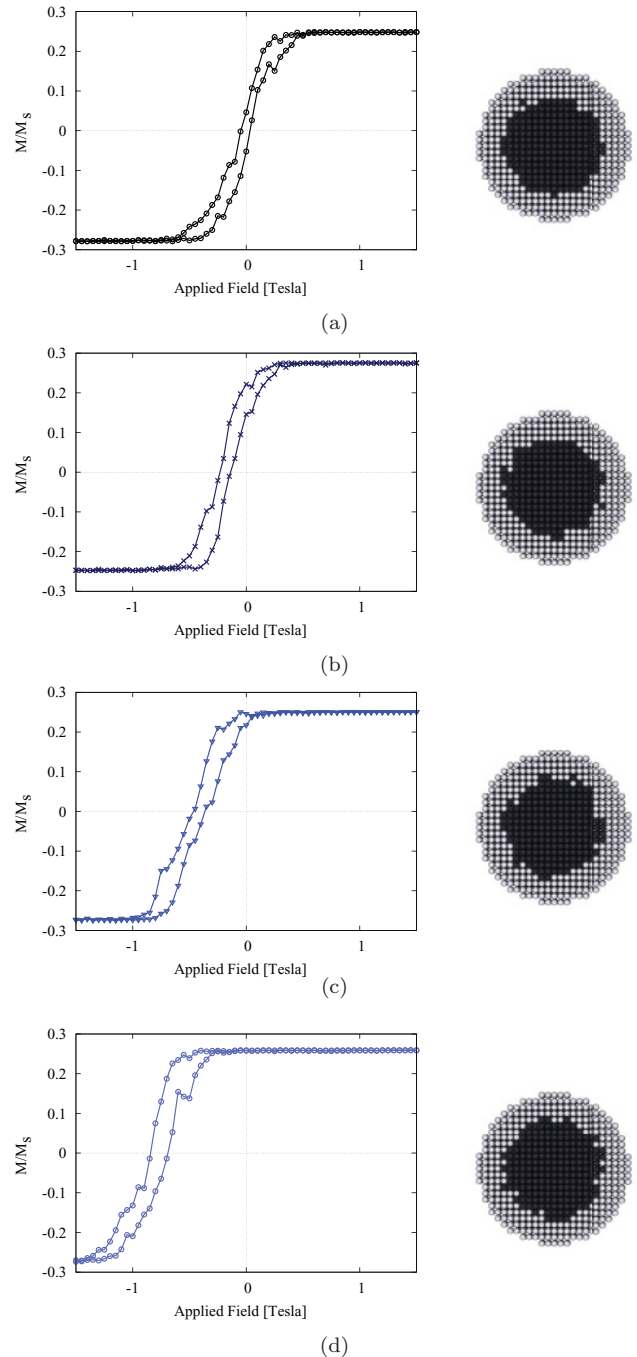


FIG. 1. (Color online) Hysteresis loops and visualizations (right) of four typical particles, each with different interfaces. Each interface structure gives rise to different hysteresis, with different degrees of exchange bias. The general trend shown in the visualizations is greater intermixing between the core and shell leads to a larger exchange-bias effect.

reverse coercivities. The roughened interface in the particles leads to wide dispersion in the exchange-bias field, and each of the modeled particles has a unique loop shape. To illustrate this dispersion, typical hysteresis loops and corresponding slices showing the internal particle structure are shown in Fig. 1 for four different generated particles (a)–(d). Exchange bias is evident in all of the examples to a varying degree. This is due to

the specific interface of each particle, and shows the sensitivity of the overall magnetic properties to changes in the interface. In general the slices show that increased roughness leads to an increase in the calculated exchange bias. Furthermore, there is a consistent trend with the simulated hysteresis loops in that they all have a small vertical shift, some greater than zero and some less than zero. This arises due to the different polarity in the AFM shell, since for these simulations an unroughened particle is uncompensated by default. The lack of compensation leads to a net *real* magnetic moment in the AFM, which is visible due to the relatively small size of the system.

In order to understand the origin of the variation of the exchange-bias field in the particles with roughened interfaces, one can return to the simple physical picture of exchange bias. If the interface between the AFM and FM is fully compensated, then if the easy axis directions are aligned no exchange bias will be present since the configuration energy of the FM is uniaxial; that is, there is no unidirectional bias field. Therefore to see significant bias one expects that some degree of the AFM interface must be *uncompensated*, which then couples with the FM. The other significant prerequisite for exchange bias is that the anisotropy in the AFM is larger than that in the FM. If not, then as the FM rotates under the effect of an external applied field, the AFM simply rotates with it. Depending on the relative values of anisotropy this can lead to an enhancement of the coercivity, but not to exchange bias. If the AFM is more directionally stable than the FM, then providing the coupling between the FM and AFM is not too strong, as the FM rotates in an applied field the exchange field from the uncompensated moment in the AFM interface leads to exchange bias. Therefore one would expect that increased roughness leads to a greater degree of uncompensation at the interface, and hence a larger degree of unidirectional coupling between the FM and AFM.

To confirm this simple physical picture, we have plotted the exchange-bias field against the net *real* magnetic moment in the AFM interface for each particle, as shown in Fig. 2. The correlation between the exchange-bias field and net moment in the AFM interface is striking. However, there is a wide dispersion in the individual exchange-bias field. The reason

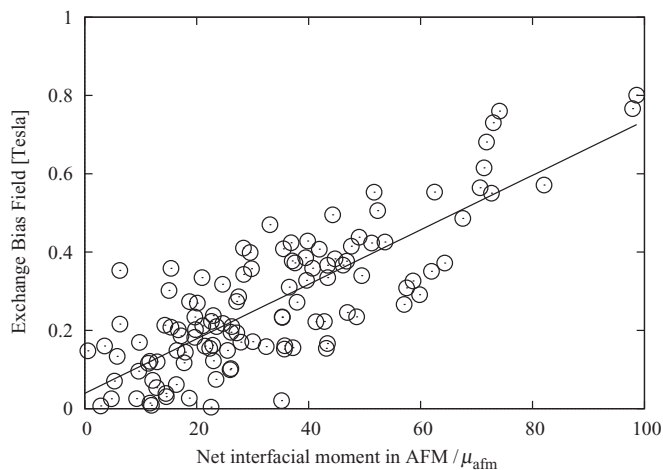


FIG. 2. Plot of the calculated exchange-bias field against the net interfacial moment in the AFM shell. Line shows a linear fit to the data.

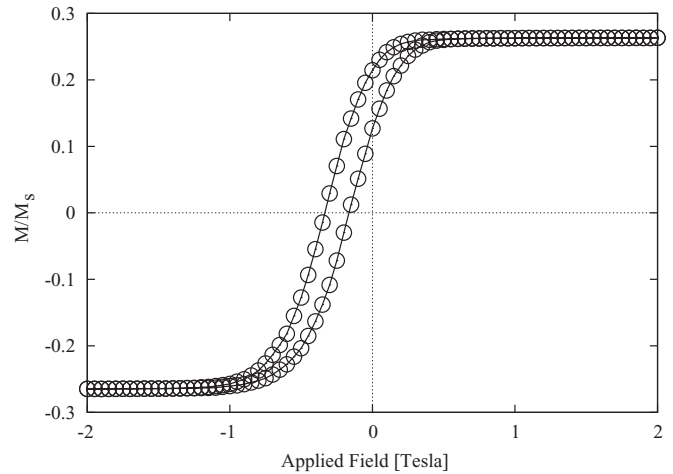


FIG. 3. Collective hysteresis loop for 128 noninteracting exchange-biased nanoparticles with aligned easy axes. The loop displays an average exchange bias but shows little relation to the individual loops of the particles. The collective loop crucially omits information regarding the statistical distribution of exchange-bias fields of individual particles.

for such a wide dispersion is not clear, but could be due to dilution of the AFM caused by isolated FM moments, or noncollinear reversal behavior of the FM at the interface (where the competing exchange interactions at the interface force certain FM moments to reverse separately from the core).

Finally we consider the overall exchange-bias effect of a collection of particles, as shown in Fig. 3. In this case the particles are noninteracting and have perfectly aligned easy axes for simplicity. The combined effect is to average out the individual hysteresis of the particles and to have an average exchange bias of approximately 0.25 T. This compares very well to the experimental results of Spasova *et al.*⁶ but it should be noted that this blurs a great deal of microscopic detail regarding the reversal process for individual particles. This illustrates that the interpretation of experimental results for exchange-biased systems must be done with care, as the overall effect of many particles can bear little resemblance to the microscopic mechanisms. The observed vertical shift of the hysteresis loops for the individual particles is not present in the collective loop due to the averaging of vertical shifts.

In conclusion, we have studied exchange-bias effects in core-shell FM-AFM nanoparticles with roughened interfaces. In reality core-shell particles do not have smooth interfaces as is often assumed in an idealistic picture of the system. We have shown that the interface roughness leads to a wide dispersion of individual exchange-bias fields, and that the magnitude of such a field is strongly correlated with the net magnetic moment in the interface of the AFM. Unlike previous studies, this net magnetic moment was created by the interface roughness and not by a value of the AFM anisotropy comparable to the exchange coupling. We have also shown that each unique particle exhibits a distinct hysteretic behavior, which emphasizes the complexity of a single particle and the necessity to study the collective behavior of a system of particles for comparison with experimental data. Because of the effect of averaging, the macroscopic hysteresis loop gives no indication of the behavior of individual grains

and gives little information on the underlying details of the magnetization reversal process.

This work was supported by the Spanish Ministry of Science and Innovation (Grant Nos. FIS2010-20979-C02-

02 and CS2008-023), Comunidad de Madrid (Grant No. S009/MAT-1726), and the European Community's Seventh Framework Programme (FP7/2007-2013) under Grant Nos. NMP3-SL-2008-214469 (UltraMagnetron) and N 214810 (FANTOMAS).

-
- ¹W. H. Meiklejohn and C. P. Bean, *Phys. Rev.* **102**, 1413 (1956).
²K. O'Grady, L. E. Fernandez-Outon, and G. Vallejo-Fernandez, *J. Magn. Magn. Mater.* **322**, 883 (2010).
³S. S. P. Parkin *et al.*, *J. Appl. Phys.* **85**, 5828 (1999).
⁴V. Skumryev, S. Stoyanov, Y. Zhang, G. Hadjipanayis, D. Givord, and J. Nogués, *Nature (London)* **423**, 850 (2003).
⁵R. F. L. Evans, R. Yanes, O. Mryasov, R. W. Chantrell, and O. Chubykalo-Fesenko, *Europhys. Lett.* **88**, 57004 (2009).
⁶M. Spasova, U. Wiedwald, M. Farle, T. Radetic, U. Dahmen, M. Hilgendorff, and M. Giersig, *J. Magn. Magn. Mater.* **272–276**, 1508 (2004).
⁷O. Iglesias, X. Batlle, and A. Labarta, *Phys. Rev. B* **72**, 212401 (2005).
⁸E. Eftaxias and K. N. Trohidou, *Phys. Rev. B* **71**, 134406 (2005).
⁹M. Kovylyna, M. García del Muro, Z. Konstantinovic, M. Varela, O. Iglesias, A. Labarta, and X. Batlle, *Nanotech.* **20**, 175702 (2009).
¹⁰M. Kiwi, *J. Mag. Magn. Mater.* **234**, 584 (2001).
¹¹R. L. Stamps, *J. Phys. D: Appl. Phys.* **33**, R247 (2000).
¹²T. C. Schulthess and W. H. Butler, *Phys. Rev. Lett.* **81**, 4516 (1998).
¹³J. Eisenmenger and I. K. Schuller, *Nat. Mater.* **2**, 437 (2003).
¹⁴J. Nogués and Ivan K. Schuller, *J. Magn. Magn. Mater.* **192**, 203 (1999).
¹⁵O. Iglesias and A. Labarta, *Physica B* **343**, 286 (2006).
¹⁶M. Pajda, J. Kudrnovský, I. Turek, V. Drchal, and P. Bruno, *Phys. Rev. B* **64**, 174402 (2001).
¹⁷M. Jamet, W. Wernsdorfer, C. Thirion, D. Mailly, V. Dupuis, P. Mélinon, and A. Pérez, *Phys. Rev. Lett.* **86**, 4676 (2001).
¹⁸D. A. Garanin, *Phys. Rev. B* **53**, 11593 (1996).
¹⁹U. Nowak, in *Annual Reviews of Computational Physics IX*, edited by D. Stauffer (World Scientific, Singapore, 2001), p. 105.
²⁰W. F. Brown, *Phys. Rev.* **130**, 1677 (1963).